

## Charmless $B$ decays in $B$ -factories

C. H. CHENG

*California Institute of Technology - 1200 East California Boulevard, Pasadena, CA 91125, USA*

(ricevuto il 29 Settembre 2011; pubblicato online il 24 Gennaio 2012)

**Summary.** — In this paper we present recent results of charmless hadronic  $B$  decays from the two  $B$ -factories,  $BABAR$  at SLAC, USA, and Belle at KEK, Japan. They include partial branching fractions of inclusive charmless  $B$  decays to  $K^+$ ,  $K^0$ , and  $\pi^+$ , branching fractions and polarizations of  $B^+ \rightarrow \rho^0 K^{*+}$ ,  $f_0 K^{*+}$ , and  $B^0 \rightarrow K^{*0} \bar{K}^{*0}$ , and branching fractions,  $CP$  asymmetries and angular distributions in  $B \rightarrow \phi\phi K$  decays.

PACS 14.40.Nd – Bottom mesons ( $|B| > 0$ ).

PACS 13.20.He – Decays of bottom mesons.

### 1. – Introduction

The dominating processes in  $B$  meson decays are through tree-level  $b \rightarrow cW^*$ , leaving a charm meson in the final states. In charmless hadronic  $B$  decays, other types of diagrams, such as  $b \rightarrow s$  penguin diagrams are enhanced. These processes allow studies of short- and long-distance QCD effects,  $CP$ -violating asymmetries, hadronic phases, and searching for evidence for physics beyond the Standard Model.

To date, approximately one hundred charmless hadronic  $B$  decay modes have been measured with more than four-sigma significance. The majority of them are from  $BABAR$  collaboration at SLAC in the United States and Belle collaboration at KEK in Japan, both of which started operation in 1999 and ended in 2008 and 2010, respectively. The branching fractions of these decay modes range from a few times  $10^{-5}$  down to  $10^{-6}$  [1]. Several other charmless channels are also searched and the upper limits of the branching fractions are well below  $10^{-6}$ .

Both  $B$ -factories,  $BABAR$  and Belle, spent most of their operation time on the  $\Upsilon(4S)$  resonance and recorded a wealth of  $B$  meson decay data through  $e^+e^- \rightarrow \Upsilon(4S) \rightarrow B\bar{B}$  processes.  $BABAR$  and Belle collected approximately  $430 \text{ fb}^{-1}$  and  $710 \text{ fb}^{-1}$  of data on  $\Upsilon(4S)$ , respectively, which corresponds to a total of more than  $1.2 \times 10^9$   $B\bar{B}$  pairs. Approximately 10% of the time they operated at about 40 MeV below the  $\Upsilon(4S)$  resonance to study non- $B$  background. They also operated at other  $\Upsilon$  resonances and scanned over an energy range above  $\Upsilon(4S)$  to higher than known resonances.

The common analysis technique amongst the analyses presented in the paper is to fully reconstruct a  $B$  meson in an event by combining all decay products of a  $B$  meson and exploiting the kinematic properties to separate signal from background. The most useful variables are energy-substituted (or beam energy-constrained) mass  $m_{ES} = \sqrt{E_{\text{beam}}^{*2} - p_B^{*2}}$  and  $\Delta E = E_B^* - E_{\text{beam}}^*$ , where the asterisk denotes the quantities evaluated in the center-of-mass (c.m.) frame,  $(E_B, p_B)$  are the energy and momentum of the reconstructed  $B$  candidate. The  $m_{ES}$  and  $\Delta E$  distributions for the  $B$  signal peak at the  $B$  meson mass and zero, respectively, and have a width of approximate 3 MeV and 30 MeV, respectively. The width of  $\Delta E$  varies in a wide range depending on the number of neutral particles in the final state. The dominant background comes from continuum events  $e^+e^- \rightarrow q\bar{q}$ , where  $q$  stands for light quarks  $u, d, s$ , or  $c$ . The topology of the continuum events is much more jet-like than the  $B\bar{B}$  events because light quarks carries much higher momentum than the  $B$  mesons. We exploit the event shape variables to build Fisher discriminant or other more sophisticated multivariate classifiers to separate signal from background. Finally, it is important to separate kaons from pions in many final states we study. Both  $B$ -factories utilize the Cherenkov radiation as the major tools to distinguish kaons from pions. The specific ionization in the tracking devices also plays a roll in particle identification.

## 2. – Inclusive charmless $B$ decays to $K^+$ , $K^0$ , and $\pi^+$

In the standard model (SM) the inclusive branching fraction of  $B$  mesons decaying to charmless final states is of the order of 2% [2]. Particles associated with physics beyond the SM, such as supersymmetric partners of SM particles, could enter the loop in  $b \rightarrow s$  and  $b \rightarrow d$  diagrams and enhance the inclusive  $b \rightarrow sg$  ( $g$  denoting a gluon) branching fraction [3, 4]. Furthermore, semi-inclusive processes are usually affected by smaller hadronic uncertainties than those that arise in calculations for exclusive final states, therefore these decays can be sensitive to non-perturbative amplitudes, such as charming penguins [5].

The signature of the inclusive charmless  $B$  decays is the presence of a light meson ( $K^+$ ,  $K_S^0$ , or  $\pi^+$ ) with momentum beyond the kinematic endpoint for  $B$  decays to charmed mesons. To suppress the overwhelming background from continuum events, one  $B$  meson is fully reconstructed through the decay modes  $B \rightarrow D^{(*)}Y^\pm$ , where  $Y^\pm$  is a combination of hadrons containing one, three, or five charged kaons or pions, up to two neutral pions, and at most two  $K_S^0 \rightarrow \pi^+\pi^-$ . After applying selections in  $m_{ES}$ ,  $\Delta E$ , and event shape variables, and fitting to  $m_{ES}$  and Fisher discriminant,  $2 \times 10^6$   $B\bar{B}$  events are reconstructed by *BABAR* from a data set of  $383 \times 10^6$   $B\bar{B}$  pairs.

From the remaining particles that does not belong to the fully reconstructed  $B$ , events that contains candidates consistent with a charm meson are rejected, and only events that contains a  $K^+$ ,  $K_S^0$  or  $\pi^+$  with a momentum  $p^*$  in the recoiled frame greater than 1.8 GeV are retained. Event yields are extracted from a maximum likelihood fit to three variables,  $m_{ES}$ , Fisher, and  $p^*$ . The probability density function (PDF) includes signal,  $q\bar{q}$ , and  $b \rightarrow c$  background components. An iterative fitting procedure is used to determine the background shapes, using events with  $p^* > 1.8$  GeV, and the signal yields at higher momentum, as shown in fig. 1. The charge  $CP$  asymmetry is also measured. The main systematic uncertainty sources include the number of fully reconstructed  $B$  candidates, efficiency estimations, PDF shapes, and  $b \rightarrow c$  background yield extrapolation.

The fitted results to the high  $p^*$  region are shown in table I. The partial branching fraction above  $p^* > 2.34$  GeV is in the range  $2\text{--}4 \times 10^{-4}$ . This results are in agree-

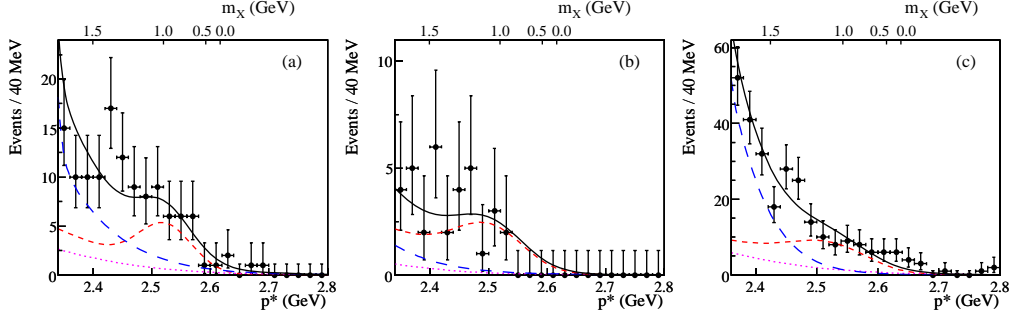


Fig. 1. – (Color online) Projection plots at high  $p^*$  for (a)  $K^+$ , (b)  $K_S^0$ , and (c)  $\pi^+$  samples [6]. The solid curves are the total fit function, the (red) dashed lines are the signal component, the (blue) long dashed are the  $b \rightarrow c$  background and the (magenta) dotted are  $q\bar{q}$ . A likelihood cut is applied to suppress the background. The scale on the upper border of the plots indicates the mass of the system recoiling against the light hadron.

ment with the estimates of the sums of known exclusive branching fractions of charmless two- and three-body  $B$  decays. On the other hand, predictions based on SCET [5] underestimate the measurements, and substantial non-perturbative charming penguin contributions or large higher-order corrections may be needed.

### 3. – $B^+ \rightarrow \rho^0 K^{*+}$ and $f_0 K^{*+}$

QCD factorization models predict a large longitudinal polarization fraction  $f_L$ , of order  $(1 - 4m_V^2/m_B^2) \sim 0.9$ , for  $B$  to two vector particles (VV) [7]. However, several measurements of penguin dominated VV final states give  $f_L \sim 0.5$  [8]. Many literatures attempt to understand the low  $f_L$  values within or beyond the SM [9].

In this section, the branching fractions, polarizations, and direct  $CP$  asymmetries of the decay modes  $B^+ \rightarrow \rho^0 K^{*+}$  (892) and  $f_0(980) K^{*+}$  measured by  $BABAR$  are summarized [10]. The measurements are based on a data sample of  $(467 \pm 5) \times 10^6$   $B\bar{B}$  pairs, and an additional  $44 \text{ fb}^{-1}$  of data collected 40 MeV below the  $\Upsilon(4S)$  is used for background studies.

The  $B^+ \rightarrow \rho^0 K^{*+}$  and  $f_0 K^{*+}$  candidates are reconstructed through the decays of  $\rho^0$  or  $f_0 \rightarrow \pi^+ \pi^-$ ,  $K^{*+} \rightarrow K_S^0 \pi^+$  or  $K^{*+} \rightarrow K^+ \pi^0$ , with  $K_S^0 \rightarrow \pi^+ \pi^-$  and  $\pi^0 \rightarrow \gamma \gamma$ . The differential decay rate for  $B^+ \rightarrow \rho^0 K^{*+}$ , after integrating over the angle between

TABLE I. – Summary of the fit results of inclusive charmless  $B$  decays [6].

	$B \rightarrow K^+ X$	$B \rightarrow K^0 X$	$B \rightarrow \pi^+ X$
Signal yield (events)	$54_{-10}^{+11}$	$32 \pm 7$	$107_{-14}^{+15}$
Significance ( $\sigma$ )	2.9	3.8	6.7
$\mathcal{B}(\times 10^{-6})_{p^* > 2.34 \text{ GeV}}$	$119_{-29}^{+32} \pm 37$	$195_{-45}^{+51} \pm 50$	$372_{-47}^{+50} \pm 59$
$A_{CP}$	$0.57 \pm 0.24 \pm 0.05$	–	$0.10 \pm 0.16 \pm 0.05$

the decay planes of the vectors is proportional to

$$(1) \quad \frac{1 - f_L}{4} \sin^2 \theta_{K^{*+}} \sin^2 \theta_{\rho^0} + f_L \cos^2 \theta_{K^{*+}} \cos^2 \theta_{\rho^0},$$

where  $\theta_{K^{*+}}(\theta_{\rho^0})$  are helicity angle of the  $K^{*+}$  ( $\rho^0$ ). The direct  $CP$  asymmetry  $A_{CP}$  is defined as  $(\Gamma^- - \Gamma^+)/(\Gamma^- + \Gamma^+)$ , where  $\Gamma^\pm = \Gamma(B^\pm \rightarrow f^\pm)$ .

Events with  $0.792 < m_{K\pi} < 0.992$  GeV,  $0.52 < m_{\pi^+\pi^-} < 1.05$  GeV,  $|\Delta E| < 10$  MeV and  $5.225 < m_{ES} < 5.289$  GeV are retained for further fit. If the final tracks can be combined to form a  $D$  candidates, the candidate is rejected. To avoid the region where the efficiency falls off rapidly,  $K^{*+}$  and  $\rho^0$  candidates need to satisfy  $\cos \theta_{K^{*+}} < 0.92$  and  $|\cos \theta_{\rho^0}| < 0.95$ , respectively. Finally a neural network discriminant is used to provide additional separation between signal and  $q\bar{q}$  background.

An extended likelihood function is used to simultaneously fit branching fractions,  $f_L$  of  $B^+ \rightarrow K^{*+}\rho^0$  and  $A_{CP}$ . The PDF uses seven variables:  $m_{ES}$ ,  $\Delta E$ , neural network output,  $m_{\pi^+\pi^-}$ ,  $m_{K\pi}$ ,  $\cos \theta_{\pi^+\pi^-}$ , and  $\cos \theta_{K\pi}$ . In the end, BABAR observes  $B^+ \rightarrow \rho^0 K^{*+}$  with a significance of  $5.3\sigma$ , and measures branching fraction  $\mathcal{B}(B^+ \rightarrow \rho^0 K^{*+}) = (4.6 \pm 1.0 \pm 0.4) \times 10^{-6}$ , the longitudinal polarization  $f_L = 0.78 \pm 0.12 \pm 0.03$ , and  $A_{CP} = 0.31 \pm 0.13 \pm 0.03$ . They also measure  $\mathcal{B}(B^+ \rightarrow f_0(980)K^{*+}) \times \mathcal{B}(f_0(980) \rightarrow \pi^+\pi^-) = (4.2 \pm 0.6 \pm 0.3) \times 10^{-6}$ , and  $A_{CP} = -0.15 \pm 0.12 \pm 0.03$ .

It is interesting to compare  $f_L$  of the three charge combinations of  $B \rightarrow \rho K^*$ :  $f_L(K^{*+}\rho^0) = 0.78 \pm 0.12 \pm 0.03$  [10],  $f_L(K^{*0}\rho^0) = 0.57 \pm 0.09 \pm 0.08$  [11],  $f_L(K^{*0}\rho^+|BABAR) = 0.52 \pm 0.10 \pm 0.04$  [11], and  $f_L(K^{*0}\rho^+|Belle) = 0.43 \pm 0.11^{+0.05}_{-0.02}$  [12].  $B^+ \rightarrow K^{*0}\rho^+$  is a pure penguin process,  $B^0 \rightarrow K^{*0}\rho^0$  is penguin plus color-suppressed  $\bar{b} \rightarrow \bar{u}u\bar{s}$  tree, and  $B^+ \rightarrow K^{*+}\rho^0$  is penguin plus color-allowed  $\bar{b} \rightarrow \bar{u}u\bar{s}$  tree. The trend of their  $f_L$  is consistent with other observations that penguin dominated processes have  $f_L \sim 0.5$  and tree dominated processes have  $f_L \sim 0.9$ .

#### 4. $B^0 \rightarrow K^{*0}\bar{K}^{*0}$ and $K^{*0}K^{*0}$

The decay  $B^0 \rightarrow K^{*0}\bar{K}^{*0}$  is a pure  $b \rightarrow d$  penguin process to two vector particles. It should have a similar longitudinal polarization fraction  $f_L$  as  $b \rightarrow s$  penguin processes under U-spin symmetry. Studying this decay mode may provide insight into the polarization puzzle in  $b \rightarrow s$  penguin dominated processes as described in the previous section, and test factorization models. If sufficient signal events are observed, a time-dependent angular analysis of  $B^0 \rightarrow K^{*0}\bar{K}^{*0}$  can distinguish between penguin annihilation and rescattering as mechanisms for the value of  $f_L$  in penguin-dominated  $B \rightarrow VV$  [13].  $B \rightarrow K^{*0}K^{*0}$  is highly suppressed in the SM, and could appear via an intermediate heavy boson beyond the SM.

BABAR uses a data sample consisting of  $383 \times 10^6$   $B\bar{B}$  pairs, and Belle uses  $657 \times 10^6$ . The analysis is very similar to that of  $B \rightarrow \rho K^*$  described in the previous section. The angular distribution is identical to equation 1 after substituting  $\rho^0$  with  $K^{*0}$ . The  $K^{*0}$  is reconstructed from  $K^{*0} \rightarrow K^+\pi^-$ , where the charge of  $K$  identifies the flavor of  $K^*$ . BABAR selects only  $0.792 < m_{K\pi} < 1.025$  GeV, while Belle keeps a larger range of  $[0.7, 1.7]$  GeV to study other resonances that contributes to  $B \rightarrow K^+\pi^- K^-\pi^+$  decays.

Events are vetoed if  $K\pi\pi$  can be combined to form a  $D^-$  meson candidate, or if  $K\pi$  can be combined to form a  $\phi$  meson candidate when the kaon mass is assigned to the pion candidate. To suppress the dominant  $q\bar{q}$  continuum background, both experiments exploit event shape variables,  $B$  candidate flight direction, and flavor tagging information.

TABLE II. – Branching fractions of  $B \rightarrow K^{*0}\bar{K}^{*0}$  and  $K^{*0}K^{*0}$ , and polarization of  $K^{*0}\bar{K}^{*0}$ .

	$\mathcal{B}(K^{*0}\bar{K}^{*0})$ ( $10^{-6}$ )	$f_L(K^{*0}\bar{K}^{*0})$	$\mathcal{B}(K^{*0}K^{*0})$ ( $10^{-6}$ )
BABAR [14]	$1.28_{-0.30}^{+0.35} \pm 0.11$	$0.80_{-0.12}^{+0.10} \pm 0.06$	$< 0.41$ at 90% C.L.
Belle [15]	$0.26_{-0.08}^{+0.33+0.10}$ ( $< 0.8$ at 90% C.L.)	—	$< 0.2$ at 90% C.L.

Both experiments use an extended unbinned maximum-likelihood fit to extract signal yields and polarization simultaneously. *BABAR* uses seven variables in their PDF:  $m_{ES}$ ,  $\Delta E$ , Fisher discriminant, and invariant masses and helicity angles of the two  $K^*$  candidates. Belle uses the product of two two-dimensional functions of  $(m_{ES}, \Delta E)$  and of the two  $K^*$  candidates invariant masses. Belle fits higher  $K^*$  resonances and  $K^*$  (892) simultaneously, while *BABAR* fits for  $K^{*0}$  (1430) contribution separately and extrapolate its contribution to  $K^*$  (892) region.

The results from both experiments are summarized in table II. The projection plots, after cutting on likelihood ratios to enhance signal component, are shown in figs. 2, 3. *BABAR* observes  $B \rightarrow K^{*0}\bar{K}^{*0}$  with a significance of  $6\sigma$ , while Belle's central value is roughly  $2\sigma$  below that of *BABAR*, and sets an upper limit below *BABAR*'s central value.

### 5. – $B \rightarrow \phi\phi K$

The three-body  $B \rightarrow \phi\phi K$  decay is a penguin  $b \rightarrow s\bar{s}s$  transition. This final state can also occur through the tree-level decay  $B \rightarrow \eta_c K$ , followed by  $\eta_c \rightarrow \phi\phi$ . The tree and penguin amplitudes may interfere at the region where the invariant mass  $m_{\phi\phi}$  is near  $\eta_c$  mass. Within the SM, the relative weak phase between these two amplitudes is very close to zero, so no  $CP$  asymmetry is expected. However, new physics contributions to the penguin loop in  $B \rightarrow \phi\phi K$  decay could introduce a non-zero relative  $CP$ -violating phase and produce a significant direct  $CP$  asymmetry [16].

The analysis techniques are very similar between Belle and *BABAR*. Both  $B^+ \rightarrow \phi\phi K^+$  and  $B^0 \rightarrow \phi\phi K^0$  are studied. In addition to  $q\bar{q}$  continuum background, possible background sources from  $B$  decays include  $B \rightarrow \phi K^+ K^- K$ ,  $B \rightarrow 5K$ ,  $B \rightarrow f_0\phi K$ , and  $B \rightarrow f_0 K^+ K^- K$ . These backgrounds can be distinguished on the  $m_{(KK)_1} - m_{(KK)_2}$

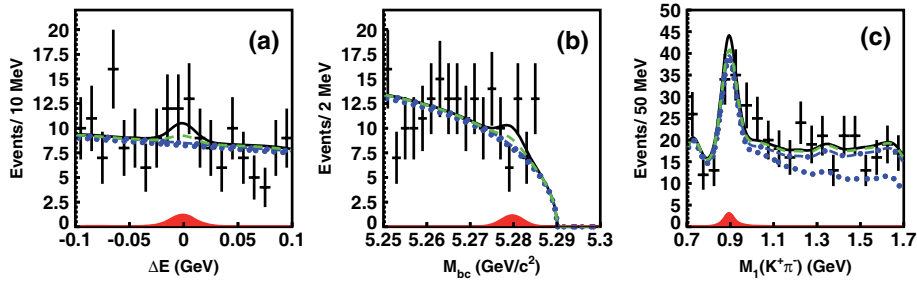


Fig. 2. – [Belle] Projections of the four-dimensional fit onto (a)  $\Delta E$ , (b)  $m_{ES}$ , and (c)  $m_{K^+\pi^-}$  and for  $B^0 \rightarrow K^{*0}\bar{K}^{*0}$  candidates. The thick solid curve shows the overall fit result; the solid shaded region represents the signal component; and the dotted, dot-dashed and dashed curves represent continuum background,  $b \rightarrow c$  background, and charmless  $B$  decay background, respectively [15].

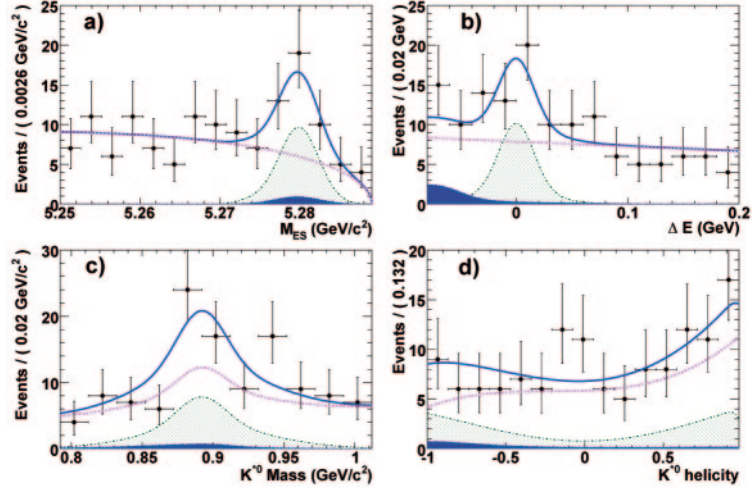


Fig. 3. – [BABAR] Projections of the fit onto (a)  $m_{ES}$ , (b)  $\Delta E$ , (c)  $K^{*0}$  mass, and (d) cosine of  $K^{*0}$  helicity angle for  $B^0 \rightarrow K^{*0} \bar{K}^{*0}$ . The solid line shows signal-plus-background; the dashed line is the continuum background; the hatched region is the signal; and the shaded region is the  $B\bar{B}$  background [14].

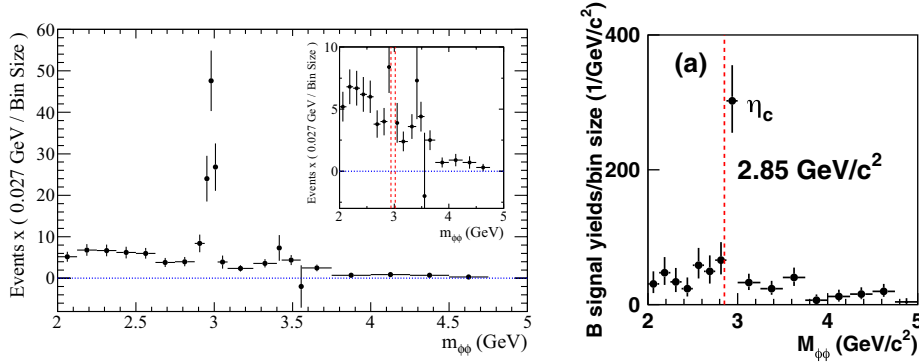


Fig. 4. – Fitted  $B^+ \rightarrow \phi\phi K^+$  yield as a function of  $m_{\phi\phi}$ . Left is from BABAR [18]; right is from Belle [17]. The inset in the left plot is the same data with an extended vertical range.

TABLE III. – Partial branching fraction of  $B \rightarrow \phi\phi K$  and direct CP asymmetry in  $B^+ \rightarrow \phi\phi K^+$ .

Partial BF ( $10^{-6}$ ) ( $m_{\phi\phi} < 2.85$ GeV)	$\mathcal{B}(B^+ \rightarrow \phi\phi K^+)$	$\mathcal{B}(B^0 \rightarrow \phi\phi K^0)$	
BABAR [18]	$5.6 \pm 0.5 \pm 0.3$	$4.5 \pm 0.8 \pm 0.3$	
Belle [17]	$3.2^{+0.6}_{-0.5} \pm 0.3$	$2.3^{+1.0}_{-0.7} \pm 0.2$	
CP Asymmetry	$m_{\phi\phi} < 2.85$ GeV	2.94–2.98 GeV	2.98–3.02 GeV
BABAR [18]	$-0.10 \pm 0.08 \pm 0.02$	$-0.10 \pm 0.15 \pm 0.02$	$-0.08 \pm 0.14 \pm 0.02$
Belle [17]	$0.01^{+0.19}_{-0.16} \pm 0.02$	$0.15^{+0.16}_{-0.17} \pm 0.02$	

plane where the two  $KK$  pairs form the two  $\phi$  candidates. Events are retained if the invariant masses of the  $\phi$  candidates are below 1.2 GeV.

Event yields are obtained by fitting with a likelihood function of  $m_{ES}$  and  $\Delta E$  ( $BABAR$  uses Fisher and two  $KK$  pair masses as well). Figure 4 shows event yields in slices of  $m_{\phi\phi}$ . Belle and  $BABAR$  find  $34 \pm 6$  ( $7 \pm 3$ ) and  $178 \pm 15$  ( $40 \pm 7$ ) signal events, respectively, for  $B^+ \rightarrow \phi\phi K^+$  ( $B^0 \rightarrow \phi\phi K^0$ ) signal events below  $m_{\phi\phi} < 2.85$  GeV. The partial branching fractions and direct  $CP$  asymmetry in regions of  $m_{\phi\phi}$  are summarized in table III. The  $CP$  asymmetry is consistent with zero, and no large deviation from the SM is found.

$BABAR$  also analyzes the angular distributions to investigate the spin components of the  $\phi\phi$  system below and within the  $\eta_c$  resonance in  $B^+ \rightarrow \phi\phi K^+$ . They find that below  $\eta_c$  the distributions are more consistent with  $J^P = 0^+$  than  $0^-$ , while within  $\eta_c$  region they are all consistent with  $J^P = 0^-$ .

## 6. – Conclusions

Charmless  $B$  decays provide a rich program in heavy flavor phenomenology and new physics search. Both  $B$ -factories continue to produce new results after the end of data taking. Partial branching fractions and  $CP$  asymmetries of inclusive  $B \rightarrow XK$ ,  $X\pi$  and  $B \rightarrow \phi\phi K$  show no evidence of new physics. More  $B$  to vector-vector final states ( $\rho^0 K^{*+}$  and  $K^{*0} \bar{K}^{*0}$ ) are studied, and more information is added to the understanding of polarization puzzle.

## REFERENCES

- [1] ASNER D. *et al.* (HFAG), “Averages of b-hadron, c-hadron, and tau-lepton Properties”, arXiv:1010.1589 (2010).
- [2] GREUB C. and LINIGER P., *Phys. Rev. D*, **63** (2001) 054025.
- [3] BIGI I. *et al.*, *Phys. Lett. B*, **323** (1994) 408.
- [4] GOKSU A., ILTAN E. O. and SOLMAZ L., *Phys. Rev. D*, **64** (2001) 054006.
- [5] CHAY J., KIM C., LEIBOVICH A. K. and ZUPAN J., *Phys. Rev. D*, **76** (2007) 094031.
- [6] DEL AMO SANCHEZ P. *et al.* (THE BABAR COLLABORATION), *Phys. Rev. D*, **83** (2011) 031103(R).
- [7] ALI A. *et al.*, *Z. Phys. C*, **1** (1979) 269; SUZUKI M., *Phys. Rev. D*, **66** (2002) 054018.
- [8] CHEN K.-F. *et al.* (BELLE COLLABORATION), *Phys. Rev. Lett.*, **94** (2005) 221804; AUBERT B. *et al.* (BABAR COLLABORATION), *Phys. Rev. Lett.*, **98** (2007) 051801; AUBERT B. *et al.* (BABAR COLLABORATION), *Phys. Rev. Lett.*, **99** (2007) 201802.
- [9] KAGAN A., *Phys. Lett. B*, **601** (2004) 151; BAUER C. *et al.*, *Phys. Rev. D*, **70** (2004) 054015; COLANGELO P. *et al.*, *Phys. Lett. B*, **597** (2004) 291; LADISA M. *et al.*, *Phys. Rev. D*, **70** (2004) 114025; LI H.-N. and MISHIMA S., *Phys. Rev. D*, **71** (2005) 054025; BENEKE M. *et al.*, *Phys. Rev. Lett.*, **96** (2006) 141801.
- [10] DEL AMO SANCHEZ P. *et al.* (THE BABAR COLLABORATION), *Phys. Rev. D*, **83** (2011) 051101(R).
- [11] AUBERT B. *et al.* (THE BABAR COLLABORATION), *Phys. Rev. Lett.*, **97** (2006) 201801.
- [12] ZHANG J. *et al.* (THE BELLE COLLABORATION), *Phys. Rev. Lett.*, **95** (2005) 141801.
- [13] DATTA A. *et al.*, *Phys. Rev. D*, **76** (2007) 034015.
- [14] AUBERT B. *et al.* (THE BABAR COLLABORATION), *Phys. Rev. Lett.*, **100** (2008) 081801.
- [15] CHIANG C.-C. *et al.* (THE BELLE COLLABORATION), *Phys. Rev. D*, **81** (2010) 071101(R).
- [16] HAZUMI M., *Phys. Lett. B*, **583** (2004) 285.
- [17] SHEN Y.-T. *et al.* (THE BELLE COLLABORATION), arXiv:0802.1547v1 (2008).
- [18] LEES J. P. *et al.* (THE BABAR COLLABORATION), *Phys. Rev. D*, **84** (2011) 012001.